BBA - Molecular Basis of Disease 1865 (2019) 165531

Contents lists available at ScienceDirect

BBA - Molecular Basis of Disease

journal homepage: www.elsevier.com/locate/bbadis

Adenovirus 36 improves glycemic control and markers of Alzheimer's disease pathogenesis

V. Hegde[a,*], M. Vijayan[b], S. Kumar[b], Md Akheruzzaman[a], N. Sawant[b], N.V. Dhurandhar[a], P.H. Reddy[b]

[a] Obesity and Metabolic Health Laboratory, Department of Nutritional Sciences, Texas Tech University, Lubbock, TX 79409, USA
[b] Internal Medicine, Cell Biology and Biochemistry, Neuroscience/Pharmacology and Neurology, Texas Tech University Health Sciences Center, Lubbock, TX 79430, USA

ARTICLE INFO

Keywords:
Glycemic control
Cognition decline
Amyloid beta
Alzheimer's disease
Ad36
APP transgenic mice

ABSTRACT

Alzheimer's disease (AD) is the most prevalent neurodegenerative disorder worldwide. While the causes of AD are unclear, several risk factors have been identified, including impaired glycemic control, which significantly increases the risk of cognitive decline and AD. In vitro and in vivo studies show that human adenovirus 36 (Ad36) improves glycemic control by increasing cellular glucose uptake in cells, experimental animal models and in humans who are naturally exposed to the virus. This study, tested improvement in glycemic control by Ad36 and delay in onset of cognitive decline in APPswe transgenic mice (Tg2576 line), a model of genetic predisposition to impaired glycemic control and AD. Three-month old APPswe mice were divided into Ad36 infected (Ad36) or mock infected (control) groups and baseline glycemic control measured by glucose tolerance test (GTT) prior to infection. Changes in glycemic control were determined 10- and 24-week post infection. Serum insulin was also measured during GTT. Cognition was determined by Y-maze test, while motor coordination and skill acquisition by rotarod test. Glycemic control as determined by GTT showed less deterioration in Ad36 infected mice over time, accompanied by a significant attenuation of cognitive decline. Analysis of brain tissue lysate showed significantly reduced levels of amyloid beta 42 in Ad36 mice relative to control mice. Golgi-Cox staining analysis also revealed reduced dendritic spines and synaptic gene expression in control mice compared to Ad36 infected mice. This proof of concept study shows that in a mouse model of AD, Ad36 improves glycemic control and ameliorates cognitive decline.

1. Introduction

Alzheimer's disease (AD) is an age dependent progressive neurodegenerative disease in which β-amyloid plaques and hyperphosphorylated tau accumulate in the brain with associated cognitive decline, dementia and eventual death [1]. AD cases are increasing with an estimated global prevalence of about 80 million predicted by 2040 [2]. While deaths from heart disease and stroke decreased by 16% and 23% respectively between 2000 and 2010, deaths due to AD increased by 68% [3]. Type 2 diabetes (T2D) is a chronic disease characterized by progressive insulin resistance (IR) and hyperglycemia with major complications including kidney disease, heart disease, retinopathy, neuropathy and cerebrovascular disease (CVD) [4,5]. Prevalence of T2D in 2013 was 410 million, a 133% increase over 13 years, the largest increase for any health condition [6]. Both T2D and AD are chronic conditions comprising an enormous public health burden. Cost of dementia care in 2014 for those over the age of 65 in the United States was around 214 billion dollars [3], only slightly less than the total estimated cost for diabetes care in 2012 at 245 billion dollars, an increase in 41% since 2007 [7].

Though aging is the strongest predictor of AD, T2D is a risk factor for developing all cause dementia and dementia attributable to AD, demonstrated in several prospective longitudinal cohort studies [8–15]. This suggests that the correction of blood sugar dysregulation may represent a crucial step in the prevention or treatment of this devastating disease.

To investigate the role of improved systemic glycemic control and its effect on ameliorating cognitive decline in a mouse model of AD, we conducted a pilot study with transgenic APP mice (Tg2576) infected with human adenovirus 36 (Ad36). Natural Ad36 infection in humans and experimental Ad36 infection of animals (chickens, rats, mice, non-human primates) is correlatively and causatively linked with obesity [16–18]. Further studies showed that Ad36 infection improves glycemic control and attenuates hepatic steatosis in rodents, despite a 60% fat

* Corresponding author at: Department of Nutritional Sciences, Texas Tech University, 1301 Akron Avenue, MS 1270, Lubbock, TX 79409, USA.
E-mail address: vijay.hegde@ttu.edu (V. Hegde).

https://doi.org/10.1016/j.bbadis.2019.08.007
Received 4 May 2019; Received in revised form 30 July 2019; Accepted 5 August 2019
Available online 06 August 2019
0925-4439/

diet [19,20]. Here we show that in APP transgenic mice susceptible to impaired glucose control and AD, Ad36 infection improves glycemic control over time and prevents cognitive decline by reducing the accumulation of soluble amyloid beta (Aβ) and preserving normal neuronal morphology.

2. Materials and methods

Transgenic amyloid beta precursor protein (APP) mice (Tg2576 mice line or APP) were generated using the mutant human APP gene 695 amino acid isoform and a double mutation (Lys670Asn and Met671Leu) (Swedish mutation). The resultant human APP transgenic mouse line exhibits an age-dependent appearance of Aβ plaques, which is confined to the cerebral cortex and the hippocampus and consistent with features of AD found in humans with AD. The APP mice begin to show cognitive impairment beginning at 6 months of age and progressing with age. The human APP transgene is maintained in the C57BL6/SJL background of these mice. Presence of the human APP transgene was determined by genotyping, in accordance with the TTUHSC Policy on Genotype Tissue Collection, using the DNA prepared from tail biopsy and PCR amplification, as described in Manczak et al. [21].

2.1. Animal experiments

The protocols for animal studies described in this study were approved by the Institutional Animal Care and Use Committee (IACUC) of the Texas Tech University Health Sciences Center. APP transgenic mice were placed on a 12 h light-dark cycle at 25 °C and individually housed in micro-isolator cages under Biosafety level-2 containment (BSL2), with ad libitum access to food and water. End of study sacrifice was conducted by cervical dislocation followed by decapitation.

2.2. Viruses

Human adenovirus Ad36 was obtained from American Type Culture Collection (ATCC cat. nos. VR913). To propagate and make viral stocks, Ad36 was plaque purified following propagation in A549 cells (human lung cancer cell line) as described [22,23] and stored at -80 °C. During the viral stock generation and handling of viral cultures strict BSL-2 safety procedures were carried out with appropriate personal protection equipment.

2.3. Glucose tolerance test

Mice were fasted for 4 h during the end of their dark cycle (feeding) period and conscious mice were injected with D-glucose (1.5 mg/kg of body weight) intraperitoneally. Tail vein blood was collected from the fasted mice prior to glucose injection (time 0) and at then at 15, 30, 60, and 120 min post-injection. Circulating blood glucose was measured using a glucometer (Breeze contour, Bayer) over time 120 min. Blood was also collected at the above mentioned time points to determine serum insulin.

2.4. ELISA for serum insulin

Serum from the tail vein and trunk blood was separated from by centrifugation at 14,000 rpm for 10 min. To determine serum insulin a microtiter plate assay (Rat/Mouse Insulin ELISA, #EZRMI-13K, Millipore) was used as per the manufacturer's instructions and the plates read at 450 nm and 590 nm absorbance on a plate reader.

2.5. Quantitative real-time PCR

During mice sacrifice, the liver was isolated, snap frozen in liquid nitrogen and stored at −80 °C. RNA was extracted from the liver tissue using RNeasy® Plus Universal Mini Kit (cat. no. 73404). Liver tissues of each mouse were dissolved (~20 mg/900 μL) in QIAzol® reagent (cat. no. 79306) and homogenized in Tissuelyser LT. Complementary DNA was synthesized with the Maxima H Minus First Strand Complementary DNA Synthesis Kit (Thermo Fisher Scientific, cat. no. K1681) from 1 μg of RNA.

Table 1
Primer sequences for genes used in qRT-PCR.

Gene name		Primer sequence (5′-3′)	GenBank accession no.
Srebp1c	Forward	GCTTCTCTTCTGCTTCTCTG	NM_001358314.1
	Reverse	GGCTGTAGGATGGTGAGT	
Chrebp	Forward	TTCCACAAGCATCCTGACT	NM_001359237.1
	Reverse	AGAAGCGTGTTCACAAGTTG	
Fasn	Forward	GTCGTCTATACCACTGCTTACT	NM_007988.3
	Reverse	ACACCACCTGAACCTGAG	
Scd1	Forward	TGCCTCTTAGCCACTGAAT	NM_009127.4
	Reverse	ACTGTTGAGATGTGAGACTGT	
Acc1	Forward	GCAGCAGTTACACCACATAC	NM_133360.2
	Reverse	TCCGCCATCTTCCACAATA	
Pepck	Forward	GACATTGCCTGGATGAAGTT	NM_011044.3
	Reverse	CGTTGGTGAAGATGGTGTT	
G6pase	Forward	GGAAGGATGGAGGAAGGAAT	NM_008061.4
	Reverse	TCAGGTCAGCAATCACAGA	
L-fabp	Forward	GTCAAGGCAGTCGTCAAG	NM_017399.5
	Reverse	ATGGTATTGGTGATTGTGTCTC	
Fatp5	Forward	AGCCAGCCATCTTATCACAT	NM_009512.2
	Reverse	AAGCAGCCAAGGAATCCA	
ApoB	Forward	TAGCAAGTTACAGAGCAGACA	NM_009693.2
	Reverse	AGTGACATCAACAGAGGAAGT	
Tnf-α	Forward	ACCACCATCAAGGACTCAA	NM_013693.3
	Reverse	AAGGTCTGAAGGTAGGAAGG	
Il-1β	Forward	TTCAGGCAGGCAGTATCA	NM_008361.4
	Reverse	CCAGCAGGTTATCATCATCATC	
Mcp-1	Forward	CTCTTCCTCCACCACCAT	NM_011333.3
	Reverse	GCTCTCCAGCCTACTCATT	
Foxo1	Forward	GCTCTGTCCTGAAGAATCCT	NM_019739.3
	Reverse	CTAATCCTGCCACTGTCTGTA	
Lipin1	Forward	GCCGTGTCATATCAGCAAT	NM_001130412.1
	Reverse	ATCGCCAGAAGTAGAGGAG	
B2m	Forward	GAAGCCGAACATACTGAACTG	NM_009735.3
	Reverse	CTGAAGGACATATCTGACATCTCT	

Srebp1c, sterol regulatory element binding protein 1c; *Chrebp*, carbohydrate response element binding protein; *Fasn*, fatty acid synthase; *Scd1*, stearoyl-Coenzyme A desaturase 1; *Acc1*, acyl CoA carboxylase 1; *Pepck*, phosphoenolpyruvate carboxykinase; *G6pase*, glucose 6-phosphatase; *L-fabp*, liver fatty acid binding protein; *Fatp5*, solute carrier family 27 (fatty acid transporter), member 5; *Apob*, apolipoprotein B; *Tnf-α*, tumor necrosis factor α; *Il-1β*, interleukin 1 β; *Mcp-1/Ccl-2*, chemokine (C−C motif) ligand 2; *Foxo1*, forkhead box O1; *B2m*, Beta-2-Microglobulin.

The expression of genes associated with liver fat metabolism was determined by quantitative real-time polymerase chain reaction (qRT-PCR). Specific primers for each gene were designed using Sigma Aldrich Oligo Architect software, listed in Table 1.

The RT-PCR reaction mix had a final volume of 20 μL; 50 ng of cDNA, 450 nM of the forward and reverse primers, and 10 μL of 1× SsoAdvanced™ Universal SYBR® Green Supermix (Bio-Rad Laboratories, cat. no. 172-5271). PCR reactions were carried out in 96-well plates using the Bio-Rad CFX RT-PCR detection system. All reactions were done in duplicates. The relative amount of all mRNAs was calculated using the $2^{-\Delta\Delta CT}$ method. Mouse *B2m* gene was used as the reference. Primer sequences for genes used in qRT-PCR are listed in Table 1.

Synaptic genes, synaptophysin (Syp) and Psd95, expression was also determined as described above. The following primers used were:

Syp (NM_009305.2)- Forward: CCTGTCCGATGTGAAGATG
Reverse: GGTGTTGAGTCCTGAAGTC
Psd95 (NM_001109752.1)- Forward: ATCCTGTCGGTCAATGGT
Reverse: AATCGGCTATACTCTTCTGGTT

2.6. Y maze

Spontaneous alternation as determined by Y-maze, tests for habituation and spatial working memory. The animal is allowed to freely explore all three arms of the Y-maze and spontaneous alternation is calculated. Total arm entries and continuous spontaneous alternation test were performed in a Y-maze (San Diego Instruments, San Diego, CA) at 12-week and 23-week post infection in uninfected control APP mice and APP mice infected with Ad36. Briefly, a mouse was placed in the Y-maze and allowed to explore for 5 min and behavior was monitored, recorded, and analyzed. A mouse was considered to have entered an arm if the whole body (except for the tail) entered the arm and to have exited if the whole body (except for the tail) exited the arm. If an animal consecutively entered three different arms, it was counted as an alternating triad. Because the maximum number of triads is the total number of arm entries minus 2, the score of alternation was calculated as "the number of alternating triads / (the total number of arm entries − 2)."

2.7. RotaRod test

Single mouse rotarod (MedAssociates, Inc.) was used to assess general motor function. Animals were placed on the rotarod one after the other facing away from the experimenter with the apparatus set to gradually increase rotation speed from 2 to 40 rpm over the course of 300 s. When the animal falls, an IR beam is broken, stopping the motor and the timer. The time for each trial was recorded, with a maximum of 300 s. Mice were then removed and following a rest of 30 min, tested for the remaining two sessions, yielding a total of three trials a day for three consecutive days. A measurement was made by monitoring latency to fall and the maximal rotation rate before the mouse fell down. To avoid any physical injury to the mouse during falls, a soft pad was placed under the equipment as a precautionary measure.

2.8. Sandwich ELISA for the soluble amyloid beta

Snap- frozen cerebral cortex from each mouse brain during sacrifice was homogenized. Briefly, protein from cortical and hippocampal tissues was homogenized in Tris-buffered saline (pH 8.0) containing protease inhibitors (20 mg/mL pepstatin A, aprotinin, phosphoramidon and leupeptin; 0.5 mM phenylmethanesulfonyl fluoride and 1 mM ethylene glycol-bis (flaminoethyl ether)-NN tetraacetic acid). Samples were briefly sonicated and centrifuged at 10,000*g* for 20 min at 4 °C. The soluble fraction was separated and used to determine soluble Aβ by ELISA. For each sample, Aβ1–40 and Aβ1–42 were measured with commercial colorimetric ELISA kits (Biosource International, Camarillo, CA, USA) specific for each species. A 96-well plate reader was used, following the manufacturer's instructions. Each sample was run in duplicate. The protein concentration of the homogenates was determined by the BSA method, and Aβ was expressed as pg Aβ/mg protein.

2.9. Immunofluorescence analysis - amyloid beta deposits

To determine the effects of Ad36 infection in Aβ deposits in APP mice, we performed immunohistochemistry and immunofluorescence analyses using the 6E10 antibody that recognizes both Aβ40 and Aβ42 deposits in uninfected control and Ad36 infected APP mice. We fixed the fresh-frozen midbrain sections (covering the hippocampus and cortex) from the control and Ad36 infected mice by dipping the sections into a 4% paraformaldehyde solution for 10 min at room temperature. The sections were incubated overnight at room temperature with the 6E10 antibody (dilution 1:400; Covance). The next day, sections were incubated with a secondary antibody conjugated with Alexa Fluor 594 (Catalog # A-21203, Invitrogen, USA) for 1 h at room temperature. The sections were washed 3 times with PBS and mounted on slides. Photographs were taken with a fluorescence microscope at 5× and 10× magnifications. Background-subtracted in the digital images and then performed quantitative analysis for deposits size and number, using NIH ImageJ.

2.10. Golgi-Cox staining and dendritic spine count

To determine normal and abnormal morphology of neurons we used Golgi-Cox impregnation. The morphology of neuronal dendrites and dendritic spines were observed in the brains of mice by Golgi-Cox staining, which was performed using the FD Rapid GolgiStain Kit (FD NeuroTechnologies, Columbia, MD, USA). Briefly, following sacrifice of the mice, brain tissue was carefully removed as quickly as possible. The intact brain tissues were rinsed with Milli Q water and impregnated with equal volumes of Solutions A and B. The impregnation solution was replaced the following day and the tissues stored at room temperature in the solution in dark for 2 weeks. Following the 2 weeks, brain tissues were transferred to Solution C. Similarly, Solution C was replaced the following day and brains further stored at 4 °C for 72 h in the dark. The Brain sections (100 μm thickness) were generated using a cryotome and the chamber temperature set at −22 °C. Each section was mounted on gelatin coated microscope slides using Solution C and excess solution removed from the slide using a Pasteur pipette and further absorbed with stacks of filter paper. The sections were allowed to dry naturally at room temperature (3 days). The dried brain sections were processed as per the manufacturer's instructions. Briefly, dendrites within the CA1 subregion of the hippocampus were imaged using a 4×, 20×, 40× and 64× objective using EVOS microscope-AMG (thermofisher.com) and Olympus1X71. Dendritic spines were detected along CA1 secondary dendrites starting from their point of origin on the primary dendrite and the counting was performed by an experimenter blinded to the group of each sample [24].

2.11. Statistical analysis

Differences in glucose clearance during GTT and insulin levels between control and Ad36 groups were analyzed by two-tailed Student's '*t*' test. Probability levels were set at $p \leq 0.05$. Multiple groups were compared using one-way ANOVA followed by Tukey's test post-hoc adjustment.

3. Results

3.1. Ad36 infection improves glycemic control in APP mice

Two month-old APP mice on chow diet (PicoLab Select Rodent 50 IF/6F 5V5R) were divided into two weight matched groups ($n = 10$ each; control and Ad36) and baseline GTT performed as described in methods, to determine blood glucose clearance. Both groups show similar glycemic control when challenged with a bolus of glucose (1.5 g/kg) (Fig. 1A–C). Following baseline GTT, mice were infected with Ad36 (1.2×10^6 PFU), or mock infected with media (control) intranasally, intraperitoneally, and orally and continued on chow diet for an additional 24 weeks.

GTT performed 10-week post infection shows faster glucose clearance in Ad36 infected mice with a 1.3-fold lower area under the curve (AUC) compared with mock-infected control mice (Fig. 1D–E), while Ad36 infected mice show better metabolic adaptability by secreting insulin to clear blood glucose (Fig. 1F). In comparison, the uninfected control mice are unable to secrete adequate insulin (Fig. 1F) displaying impaired glucose clearance (Fig. 1D–E).

The Ad36 infected mice continue to clear blood glucose faster than the control mice even after 24-weeks post infection with a 1.25-fold lower AUC (Fig. 1G–H) compared with control mice. Both groups of mice appear to secrete similar amounts of insulin in response to the glucose challenge (Fig. 1I), which is higher than the baseline or 10-week post infection.

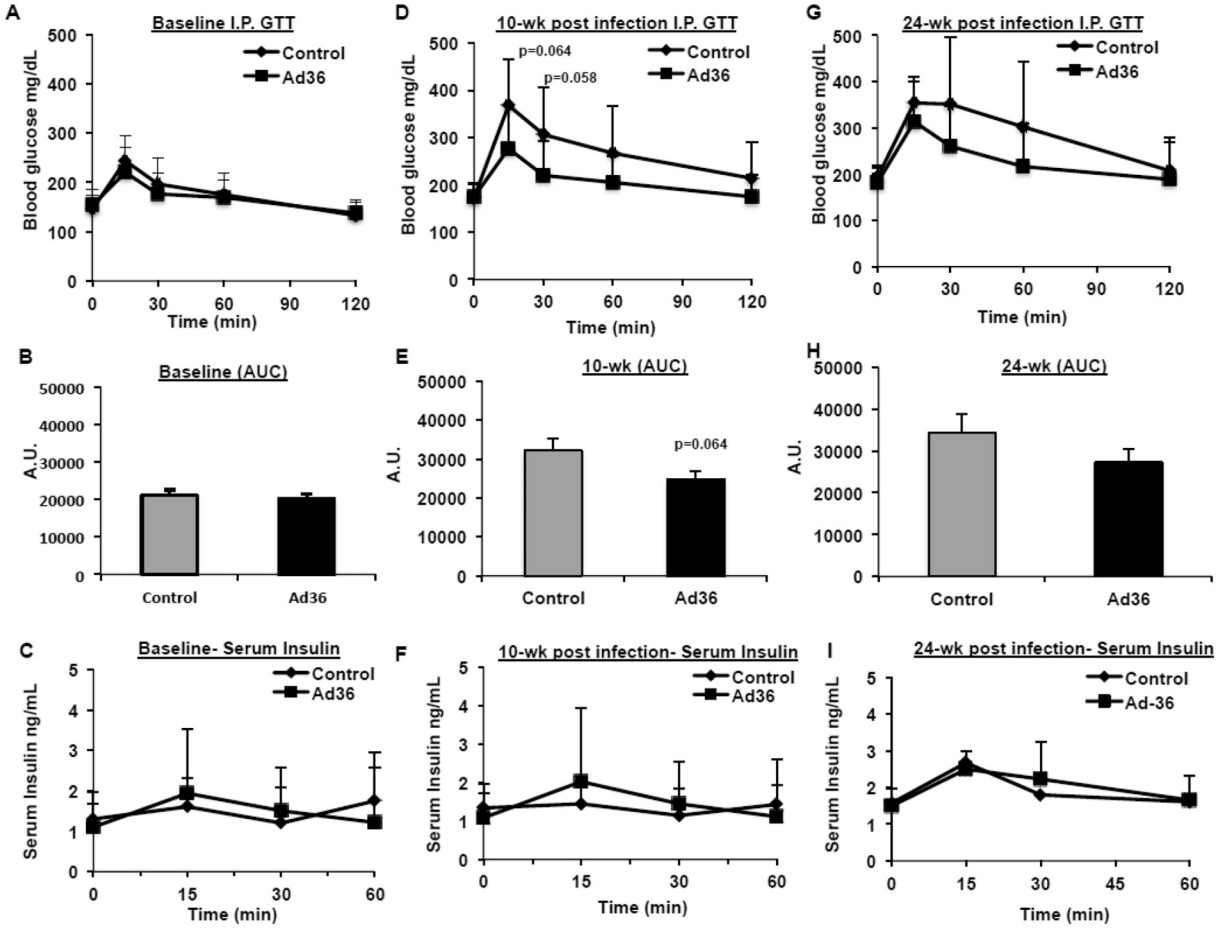

Fig. 1. Ad36 infection improves glycemic control in APP mice. Transgenic APP mice (Tg2576 mice line) infected with Ad36 show improved glycemic control as measured by glucose clearance during GTT compared with control uninfected mice. (A) Baseline GTT and (B) corresponding AUC and (C) serum insulin during GTT is shown. GTT performed 10-weeks post infection (D) and 24-weeks post infection (G) is shown with their respective AUC (E and H) and corresponding serum insulin levels (F and I).

3.2. Ad36 infection reduces deterioration of glycemic control in APP mice

Improvement in glucose metabolism was further determined by comparing the change in glycemic control over the 24 weeks post infection with Ad36. When compared between groups, the AUC shows a significant deterioration from baseline to 24 weeks in the control mice (Fig. 2A), while Ad36 infected APP mice do not show any significant change in glycemic control from baseline to 10 weeks post infection or 24 weeks post infection (Fig. 2A). Comparison between 10-week and 24-week AUC does not show any difference between the groups (Fig. 2A). As seen in Fig. 2B, when we compared within the groups, in control mice, the glycemic control deteriorated over the 24 weeks from baseline. The AUC for GTT in control mice increased significantly at 10-weeks and at 24-weeks (Fig. 2B) over baseline. In comparison, Ad36 infected mice, did not display any significant increase in AUC at 10-weeks and at 24-weeks (Fig. 2B) over baseline. The percent change over time measured as a difference (delta) from baseline, control mice showed greater percent change at 10-weeks (17.2%) and at 24-weeks (49.7%) compared with Ad36 infected mice at 10-weeks (10.7%) and at 24-weeks (28%) respectively.

3.3. Ad36 protects the liver from increased fatty acid transport

We determined if improvement in systemic glycemic control caused changes in liver metabolism. Using quantitative real time PCR (qRT-PCR) analysis we measured RNA expression of genes involved in liver de novo lipogenesis, fatty acid transport, inflammation and gluconeogenesis. Liver de novo lipogenesis genes sterol regulatory element-binding protein 1c (Srebp1c), fatty acid synthase (Fasn) and acetyl CoA carboxylase (Acc1) did not show any difference between Ad36 infected and uninfected control mice (Fig. 3A). The carbohydrate responsive-element binding protein (Chrebp) however showed significantly increased expression in Ad36 infected mice compared with control mice (Fig. 3A). Further, we determined the expression of genes in the fatty acid transport into the liver, namely fatty acid binding protein (L-FABP), fatty acid transport protein-5 (Fatp-5) and apolipoprotein B (ApoB). As seen in Fig. 3B, gene expression for all three genes is significantly down regulated in Ad36 infected mice compared with control mice (Fig. 3B). Inflammatory genes, tumor necrosis factor-α (Tnf-α), monocyte chemoattractant protein-1 (Mcp-1) and interleukin-1β (IL-1β) did not show any difference in expression between the Ad36 infected and uninfected control mice (Fig. 3C). We also determined the expression of genes involved in the gluconeogenesis pathway. Fig. 3D shows that phosphoenolpyruvate carboxykinase (Pepck), glucose-6-phosphatase (G6Pase), forkhead box O1(Foxo-1) and Lipin-1 did change in expression between Ad36 infected and control mice (Fig. 3D). But stearoyl-CoA-desaturase-1 (Scd-1) gene expression was significantly lower in Ad36 mice compared with control mice (Fig. 3D).

3.4. Ad36 infection prevents cognition decline in APP mice

(a) Y-Maze

During the 5 min test session in a Y-maze, APP mice infected with

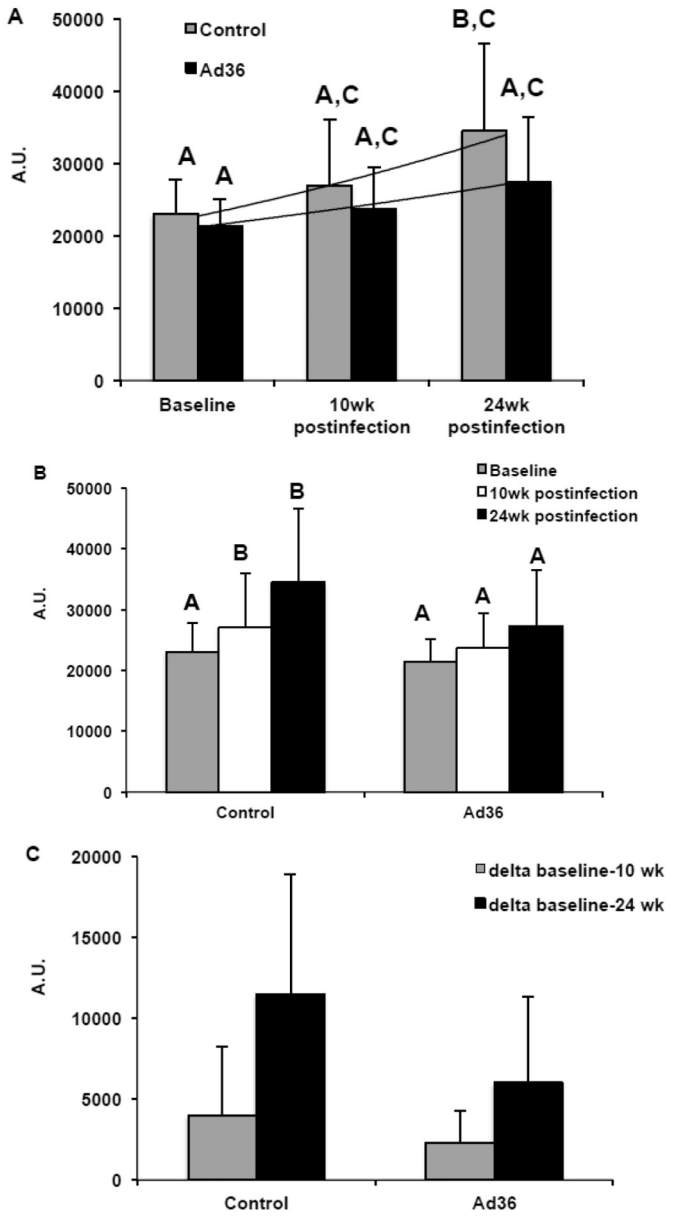

Fig. 2. Ad36 infection reduces deterioration of glycemic control in APP mice. (A) The AUC, when compared between groups, shows a significant deterioration from baseline to 24 weeks in control mice, while Ad36 infected mice do not show any significant change in glycemic control from baseline to 10 weeks post infection or 24 weeks post infection. Groups not sharing an alphabet are significantly different. (B) Compared to baseline, control uninfected mice show significantly higher deterioration in glycemic control over 24 weeks compared with Ad36 infected mice. Groups not sharing an alphabet are significantly different. (C) The difference in glycemic control between baseline and 10-weeks or 24-weeks was also higher in control mice compared with Ad36 infected mice.

Ad36 had a significantly higher probability of alternating three consecutive entries than uninfected control APP mice at 12-week and 23-week post infection (Fig. 4 B and D respectively). This result suggested that the spatial working memory of Ad36 treated APP mice was enhanced compared with untreated APP mice. We also analyzed the total number of arm entries. Ad36 infected mice had significantly more total arm entries than uninfected control mice at 12-week ($p = 0.003$; Fig. 4A) and 23-week post infection ($p = 0.01$; Fig. 4C), suggesting increased general activity in Ad36 infected mice.

(b) Rotarod test

Rotarod, motor coordination and motor skill acquisition were determined in control and Ad36 infected mice. As seen in Fig. 4E–F, Ad36 infected mice show a 1.6-fold lower latency to falls, indicating less impairment in motor learning and coordination compared to control mice due to mutant APP expression.

3.5. Ad36 infection reduces amyloid beta-40 and 42 levels and deposits in APP mice

Abnormal APP level and amyloid beta toxicities are the key factors responsible for amyloid pathology and cognitive decline in APP mice and AD. We determined the levels of amyloid beta-40 and 42 protein in the cerebral cortex of APP control mice ($n = 4$) and Ad36 infected APP mice ($n = 4$). Sandwich ELISA analysis of tissue lysate showed significantly reduced levels of amyloid beta 42 ($p = 0.0007$) in APP mice infected with Ad36 relative to uninfected control APP mice (Fig. 5A). The tissue level of amyloid beta 40 was also found to be decreased in Ad36 infected APP mice ($p = 0.07$; Fig. 5A) compared to control APP mice, although it was not significant.

As shown in Fig. 5B, immunohistochemistry staining of Aβ deposits shows distinctly lower presence of Aβ plaques in Ad36 infected APP mice compared with control mice. Upon quantification, we found significantly fewer Aβ plaques in the hippocampus/cortical sections ($p = 0.0023$; Fig. 5C) of Ad36 infected APP mice, relative to the uninfected control mice. We also found the size of Aβ plaques to be significantly smaller in the Ad36 infected APP mice ($p = 0.0003$; Fig. 5D), compared with the uninfected control mice. These observations strongly suggest that Ad36 infection reduces amyloid number and size in APP mice.

3.6. Ad36 infection maintains dendritic spine morphology and prevents reduction of synaptic proteins

To determine the effects of Ad36 on dendritic length and spines, we quantified dendritic length and number of spines using Golgi-Cox staining in hippocampus of 24 weeks uninfected APP and Ad36 treated APP mice. As shown in Fig. 6A, we found significantly increased dendritic length in Ad36 infected APP mice ($p = 0.0001$) relative to control mice. We also found significantly increased number of dendritic spines in Ad36 infected APP mice ($p = 0.0001$) compared with control mice. These observations indicate that Ad36 infection enhances both dendritic length and number of dendritic spines in APP mice.

Next to determine the effect of Ad36 infection on synaptic proteins, we quantified gene expression of synaptophysin and PSD95 from hippocampal tissues. Quantitative real time PCR analysis showed that synaptophysin gene expression was significantly increased in Ad36 infected mice ($p = 0.029$) compared uninfected control mice (Fig. 6B), however, PSD95 expression was not significantly different between the two groups of APP mice (Fig. 6B).

4. Discussion

Many epidemiological and clinical studies have shown that AD patients often exhibit impairment in glucose and/or insulin regulation, and that T2D is the second greatest risk factor for AD [25–31]. Furthermore, cognitive decline as well as amyloidosis and tau pathology has been observed in the brains and pancreas of diabetic patients [32–34]. This suggests that a pre-diabetic impairment in peripheral glucose and insulin regulation contributes to AD pathogenesis. In mice, experimental infection with human adenovirus Ad36 significantly improves systemic glycemic control in chow fed animals [19,35] and improves hyperglycemia and hepatic steatosis induced by high-fat diet, without requiring a reduction in adiposity [35]. Therefore, in this study, we investigated how improvement in peripheral glycemic control by Ad36 in a mouse model of APP modulates cognition decline, amyloid beta levels and morphology of neuronal dendrites and

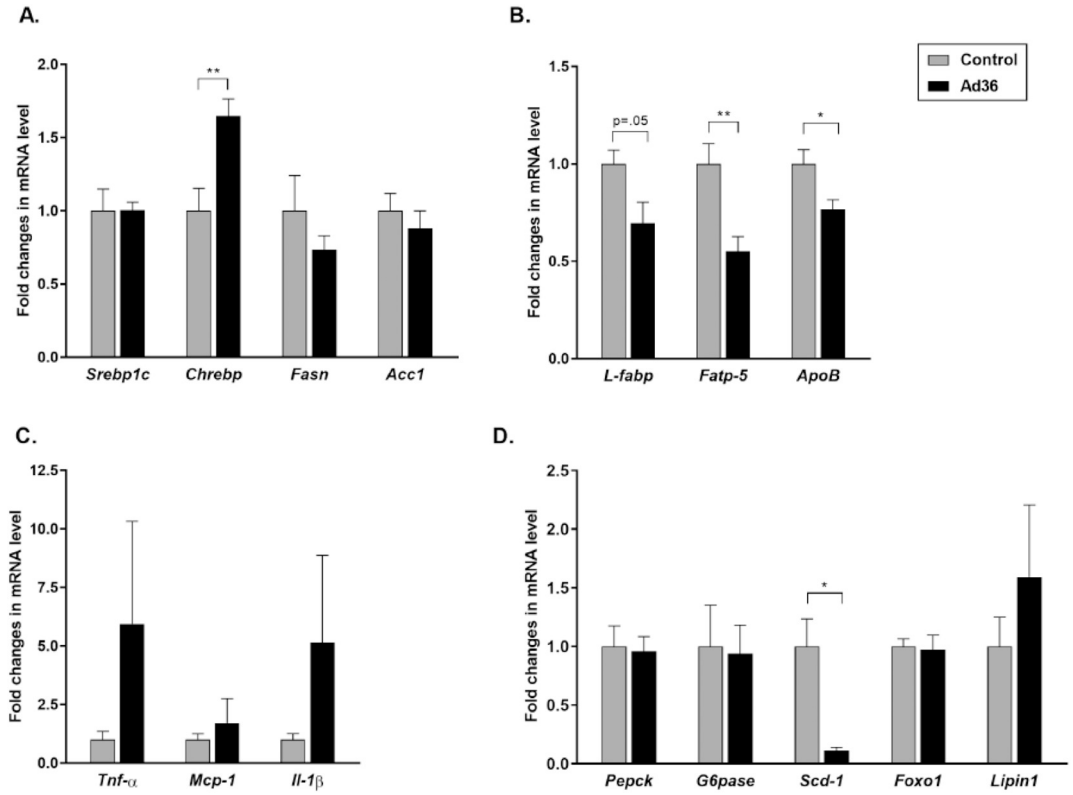

Fig. 3. Ad36 protects liver from increased fatty acid transport. Liver metabolism was determined by measuring RNA expression of genes involved in liver (A) de novo lipogenesis, (B) fatty acid transport, (C) inflammation and (D) gluconeogenesis.

dendritic spines in the brain.

In mice models of AD, the association of peripheral glucose regulation in the development of AD neuropathology and cognitive decline is not clear. There are several inconsistencies among the different models regarding the age and timing of observed glucose impairment [36–43]. Recently, two different transgenic mice studies showed that a pre-diabetic phenotype is present in these mice, which occurs prior to detection of AD related pathogenesis [44,45]. In APP mice, Ad36 infection improved glucose clearance 10 weeks (Fig. 1A–B) and 24 weeks (Fig. 1G–H) post infection compared with uninfected control mice. The improvement in glucose clearance was variable from 10-weeks to 24-weeks, with more significant improvement observed at 10-weeks compared with 24-weeks. A possible explanation is that Ad36 is a human adenovirus and its infection in mice is abortive in nature, hence we expect to observe a decline in the effect of Ad36 over time. Further, compared to baseline, the control mice had progressively significant deterioration in glycemic control over 24 weeks (Fig. 2A–C), while no significant difference was observed with Ad36 infected APP mice (Fig. 2A–C). In humans, beyond its accepted role in whole body metabolism regulation [46], insulin also modifies neuronal activity promoting synaptic plasticity [47,48] and improves memory function in the mammalian brain [49,50]. Several studies have suggested that IR in the brain directly promotes the development of beta-amyloid (Aβ) and tau pathologies seen during AD [31,51]. IR in the brain may also aggravate pre-existing AD pathology by promoting Aβ and tau pathology and is known to be associated with cognitive decline independently of AD pathology [52,53].

The amyloid precursor protein (APP), a large transmembrane protein, is cleaved by sequential β and γ secretase to form several peptides between 39 and 43 amino acids in length known as Aβ. Among the histopathological hallmarks of AD, most common are aberrant oligomerization of certain Aβ peptides (such as Aβ42) and extracellular plaques formed with Aβ fibrils at their center in equilibrium with soluble oligomers [54–57]. Ad36 infection showed significantly reduced levels of amyloid beta 42 ($p = 0.0007$) in the cerebral cortex tissue lysate relative to uninfected control APP mice (Fig. 5A). Although not significant, tissue level of amyloid beta 40 was also found to be decreased in Ad36 infected APP mice ($p = 0.07$; Fig. 5A). Immunohistochemistry staining of Aβ deposits showed distinctly lower presence of Aβ plaques (Fig. 5B), with significantly fewer and smaller Aβ plaques (Fig. 5C and D respectively) in Ad36 infected APP mice compared with control mice. These observations strongly suggest that human adenovirus Ad36 might have some molecular interaction with APP protein and reduces amyloid number and size in APP mice. Alternatively, Ad36 might facilitate amyloid beta clearance, which needs to be investigated further. Synaptic damage in AD neurons has been shown to be induced by amyloid beta accumulations at synapses [58,59]. However the fundamental and specific cellular changes are not completely understood. Growing evidence suggests that in AD patients and AD mice, dendritic spine density is critical for synaptic function and cognitive behavior [60,61]. In this study, using Golgi-Cox staining in hippocampus of uninfected APP and Ad36 treated APP mice at 9–10 months of age, as seen in Fig. 6A, we found significantly increased dendritic length ($p = 0.0001$) and number of dendritic spines ($p = 0.0001$) in Ad36 infected APP mice relative to uninfected control mice. These observations indicate that Ad36 infection enhances both dendritic length and number of dendritic spines in APP mice. Further, Ad36 infection increased expression of the synaptic gene synaptophysin while PSD95 did not show any significant changes (Fig. 6B). The cognitive defects are caused by changes in the structure and function of synapse as well as frank synapse with accompanied neuronal loss, which contributes to the neural system dysfunction [61]. Cognitive tests showed that APP mice infected with Ad36 had a significantly higher spatial working memory compared with untreated APP mice as determined by Y-maze (Fig. 4B and D). Ad36 infected mice also displayed significantly more total arm entries than uninfected control mice (Fig. 4A and C) suggesting increased general activity in Ad36 infected mice. On an accelerating rotarod test, APP mice displayed reduced

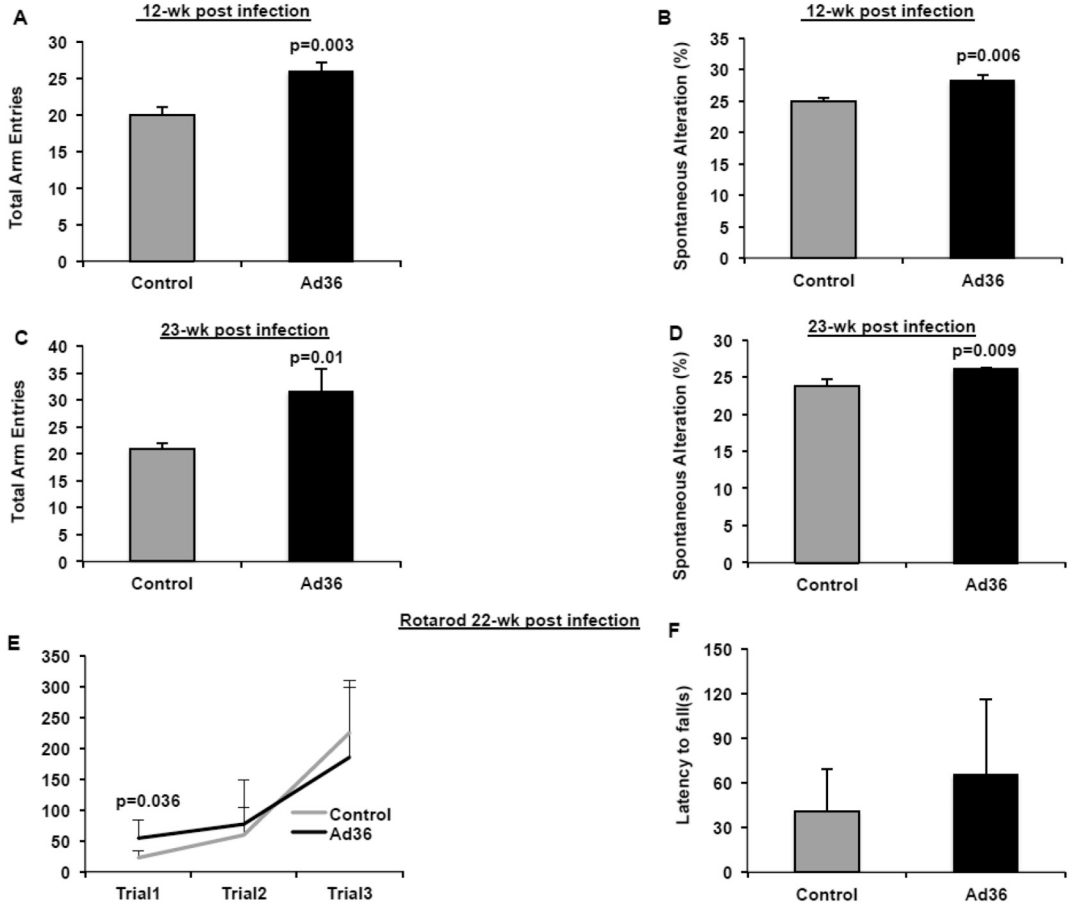

Fig. 4. Ad36 infection prevents cognition decline in APP mice. Difference in cognition was measured via the Y-maze and Rotarod analysis. Y-maze test shows APP mice infected with Ad36 display significantly more total arm entries than uninfected control mice at 12-weeks post infection (A) and 23-weeks post infection (C) along with significantly higher spatial working memory at 12-weeks post infection (B) and 23-weeks post infection (D). Control uninfected mice also showed reduced latency to fall (F) on an accelerating rotarod test during 3 independent trials (E) compared with Ad36 infected mice at 22-weeks post infection.

latency to fall relative to Ad36 infected mice (Fig. 4E and F), indicating that impairments in motor learning and coordination. Collectively, these observations suggest that improvement in glycemic control by Ad36 infection prevents degeneration of dendritic spine structure, synaptic function, and cognition. In rodent models, Ad36 infection has shown presence of viral DNA in the brain ([77]) and Ad36 infection affects hypothalamic monoamines and stress axis [19], which is suggestive of a role for Ad36 in modifying brain activity.

Anti-diabetic medication metformin, and other hypoglycemic medications [62,63], have been shown to significantly improve health- and lifespan. Although inconsistent, monotherapy with insulin [64,65] or treatment with other glucose lowering medications [66,67] has shown some improvement in memory performance in non-diabetic AD patients and slowing of AD symptom progression. Other studies have shown that compared with elderly individuals without T2D, similar people with T2D who are treated with insulin plus other hypoglycemic agents (i.e., combination therapy) have dramatically less AD neuropathology (reduced densities of neuritic plaques and neurofibrillary tangles in the cortex) [68]. These studies underscore the importance of insulin or other anti-diabetic medications as possible treatments for T2D associated AD pathology. However, insulin and several of the anti-diabetic drugs depend on a functional insulin-signaling pathway, which is often impaired during insulin resistance or T2D. Therefore, a therapeutic agent, like Ad36, which can improve glycemic control independent of insulin or the impaired proximal insulin signaling pathway [20,69] is very attractive to improve peripheral glycemic control and AD associated pathology.

Adenovirus 36 is a commonly occurring infection in humans [18]. Natural Ad36 infection is associated with better glycemic control in humans [20]. A longitudinal study of 1500 middle-aged subjects followed for 10 years showed that at baseline, those individuals who were naturally infected with Ad36 had significantly less deterioration in glycemic control after 10 years, compared to the uninfected individuals [76]. It would be interesting to determine if the presence of natural Ad36 infection is linked with less cognitive impairment in humans. Also, it would be important to determine Ad36 infection status as a covariate in estimating AD risk in humans.

5. Conclusion

This proof of concept study shows that in a mouse model predisposed to impaired glycemic control and AD, Ad36 improves glycemic control and ameliorates cognitive decline. Additional and long-term research is needed to determine if Ad36-based approaches may help in improving the prognosis of AD. This study also opens up a new angle for epidemiological investigation of the potential role of Ad36 in reducing AD risk.

Transparency document

The Transparency document associated with this article can be

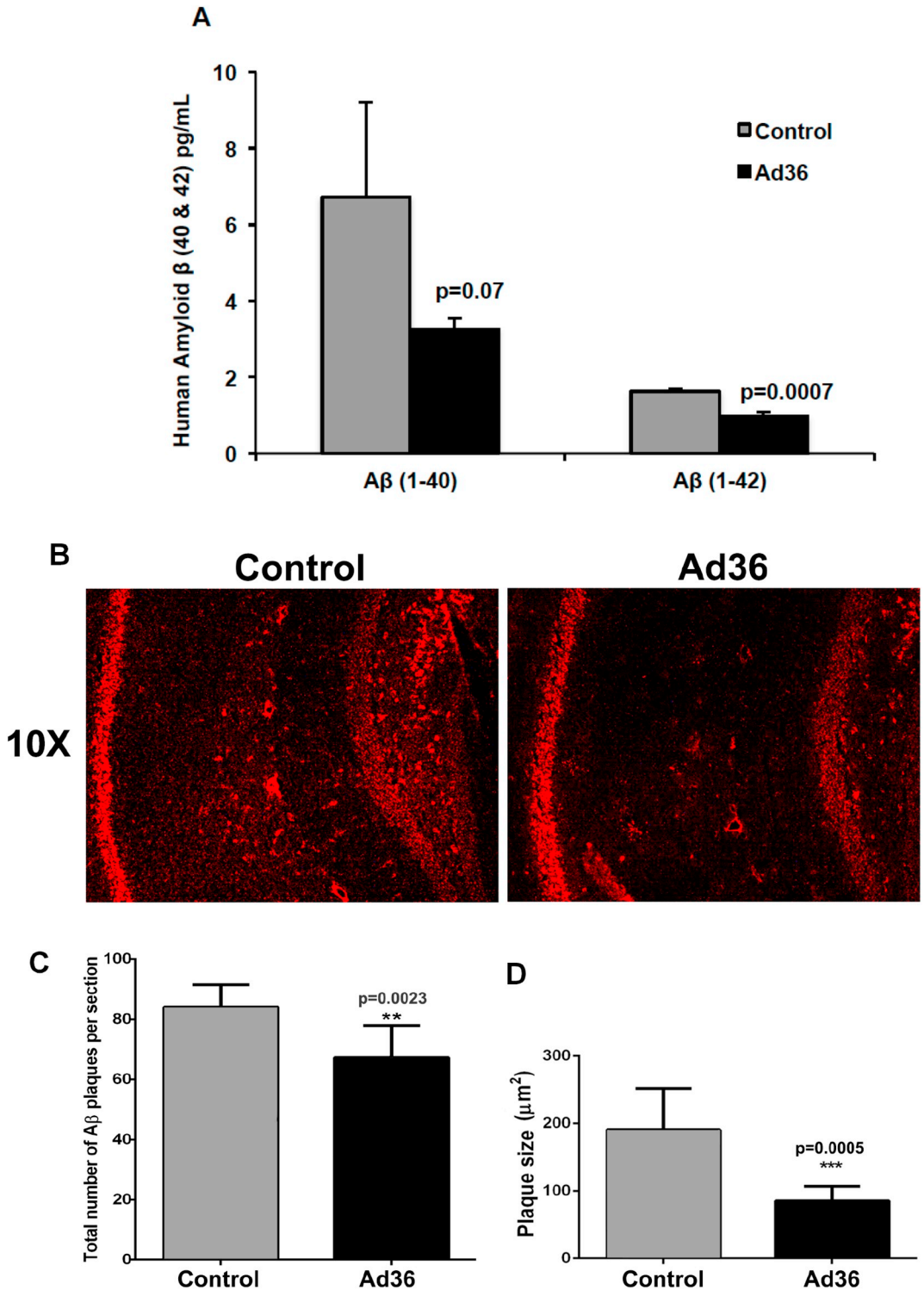

Fig. 5. Ad36 infection reduces Amyloid beta-40 and 42 levels and deposits in APP mice. (A) Ad36 infection shows significantly reduced levels of amyloid beta 42 (p = 0.0007) in the cerebral cortex tissue lysate relative to uninfected control APP mice. Amyloid beta 40 was also found to be decreased in Ad36 infected APP mice (p = 0.07). (B) Immunofluorescence analysis of Aβ deposits shows lower presence of Aβ plaques in Ad36 infected mice. (C) These mice show significantly fewer Aβ plaques in the hippocampus/cortical sections (p = 0.0023) and (D) significantly smaller Aβ plaques to be in the Ad36 infected APP mice (p = 0.0003), compared with the uninfected control mice.

found, in online version.

Funding

The study was supported by a grant from the Texas Tech University President's collaborative grant to VH and PHR.

Declaration of competing interest

NVD has received several United States and international patents that protect intellectual property about the use of adenoviruses and its proteins in obesity, diabetes and related areas.

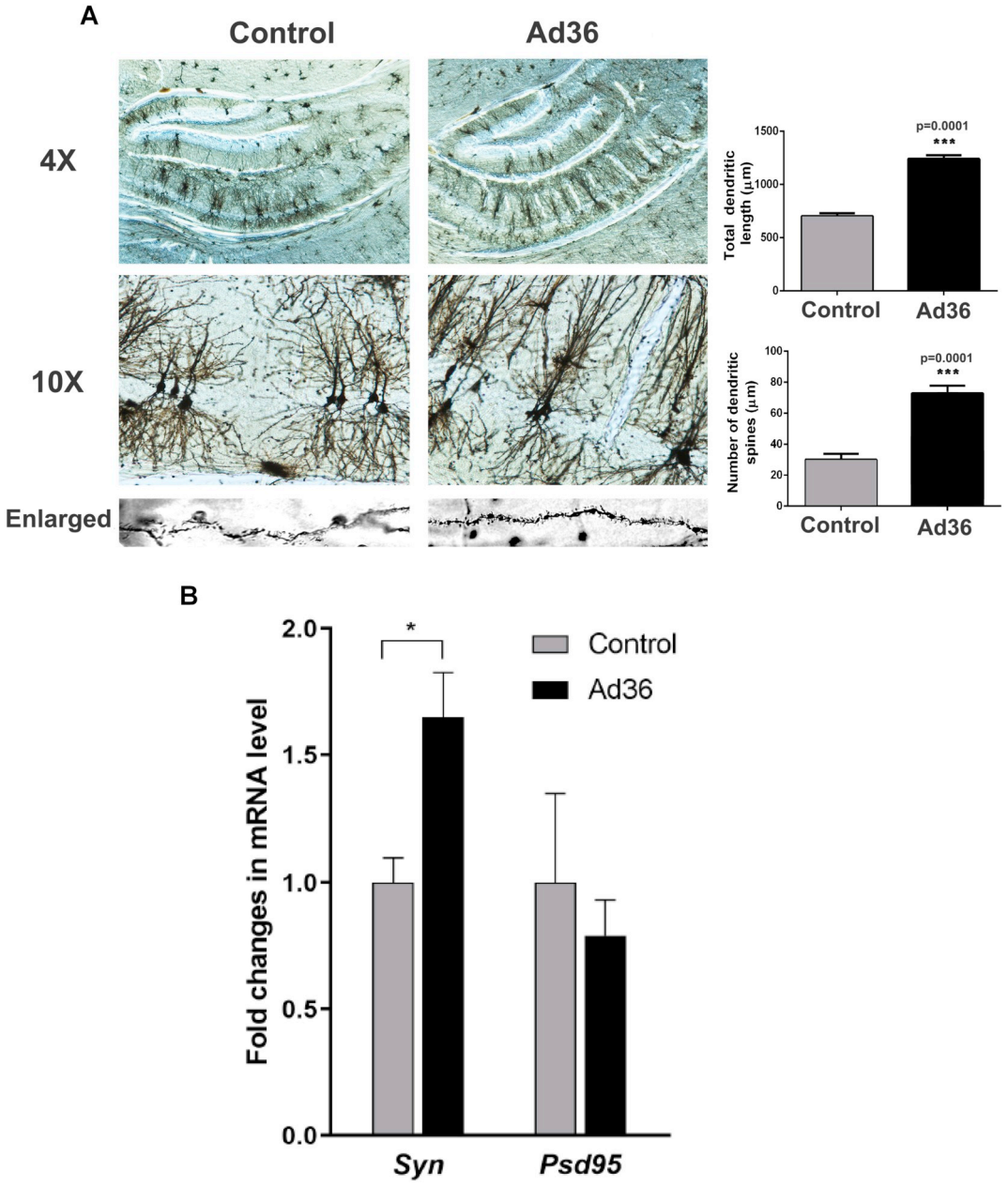

Fig. 6. Ad36 infection maintains Dendritic Spine morphology and prevents reduction of synaptic proteins. (A) Hippocampal dendritic spine density is reduced in control mice compared with Ad36 infected mice but dendritic length and number of dendritic spines was significantly increased in Ad36 infected APP mice ($p = 0.0001$ and $p = 0.0001$ respectively) compared with control mice. (B) Ad36 infection significantly increases gene expression for synaptic gene synaptophysin compared with uninfected control mice at 24-weeks post infection.

Appendix A. Supplementary data

Supplementary data to this article can be found online at https://doi.org/10.1016/j.bbadis.2019.08.007.

References

[1] C. Ballard, S. Gauthier, A. Corbett, C. Brayne, D. Aarsland, E. Jones, Alzheimer's disease, Lancet 377 (2011) 1019–1031.
[2] C.P. Ferri, M. Prince, C. Brayne, H. Brodaty, L. Fratiglioni, M. Ganguli, K. Hall, K. Hasegawa, H. Hendrie, Y. Huang, A. Jorm, C. Mathers, P.R. Menezes, E. Rimmer, M. Scazufca, I. Alzheimer's Disease, Global prevalence of dementia: a Delphi consensus study, Lancet 366 (2005) 2112–2117.
[3] A. Alzheimer's, 2014 Alzheimer's disease facts and figures, Alzheimers Dement. 10 (2014) e47–e92.
[4] A.D. Deshpande, M. Harris-Hayes, M. Schootman, Epidemiology of diabetes and diabetes-related complications, Phys. Ther. 88 (2008) 1254–1264.
[5] F. Zaccardi, D.R. Webb, T. Yates, M.J. Davies, Pathophysiology of type 1 and type 2 diabetes mellitus: a 90-year perspective, Postgrad. Med. J. 92 (2016) 63–69.
[6] G.B.D.R.F. Collaborators, M.H. Forouzanfar, L. Alexander, H.R. Anderson, V.F. Bachman, S. Biryukov, M. Brauer, R. Burnett, D. Casey, M.M. Coates, A. Cohen, K. Delwiche, K. Estep, J.J. Frostad, K.C. Astha, H.H. Kyu, M. Moradi-Lakeh, M. Ng, E.L. Slepak, B.A. Thomas, J. Wagner, G.M. Aasvang, C. Abbafati, A. Abbasoglu Ozgoren, F. Abd-Allah, S.F. Abera, V. Aboyans, B. Abraham, J.P. Abraham, I. Abubakar, N.M. Abu-Rmeileh, T.C. Aburto, T. Achoki, A. Adelekan, K. Adofo, A.K. Adou, J.C. Adsuar, A. Afshin, E.E. Agardh, M.J. Al Khabouri, F.H. Al Lami, S.S. Alam, D. Alasfoor, M.I. Albittar, M.A. Alegretti, A.V. Aleman, Z.A. Alemu, R. Alfonso-Cristancho, S. Alhabib, R. Ali, M.K. Ali, F. Alla, P. Allebeck, P.J. Allen, U. Alsharif, E. Alvarez, N. Alvis-Guzman, A.A. Amankwaa, A.T. Amare, E.A. Ameh, O. Ameli, H. Amini, W. Ammar, B.O. Anderson, C.A. Antonio, P. Anwari, S. Argeseanu Cunningham, J. Arnlov, V.S. Arsenijevic, A. Artaman, R.J. Asghar, R. Assadi, L.S. Atkins, C. Atkinson, M.A. Avila, B. Awuah, A. Badawi, M.C. Bahit, T. Bakfalouni, K. Balakrishnan, S. Balalla, R.K. Balu, A. Banerjee, R.M. Barber, S.L. Barker-Collo, S. Barquera, L. Barregard, L.H. Barrero, T. Barrientos-Gutierrez, A.C. Basto-Abreu, A. Basu, S. Basu, M.O. Basulaiman, C. Batis Ruvalcaba, J. Beardsley, N. Bedi, T. Bekele, M.L. Bell, C. Benjet, D.A. Bennett, H. Benzian,

E. Bernabe, T.J. Beyene, N. Bhala, A. Bhalla, Z.A. Bhutta, B. Bikbov, A.A. Bin Abdulhak, J.D. Blore, F.M. Blyth, M.A. Bohensky, B. Bora Basara, G. Borges, N.M. Bornstein, D. Bose, S. Boufous, R.R. Bourne, M. Brainin, A. Brazinova, N.J. Breitborde, H. Brenner, A.D. Briggs, D.M. Broday, P.M. Brooks, N.G. Bruce, T.S. Brugha, B. Brunekreef, R. Buchbinder, L.N. Bui, G. Bukhman, A.G. Bulloch, M. Burch, P.G. Burney, I.R. Campos-Nonato, J.C. Campuzano, A.J. Cantoral, J. Caravanos, R. Cardenas, E. Cardis, D.O. Carpenter, V. Caso, C.A. Castaneda-Orjuela, R.E. Castro, F. Catala-Lopez, F. Cavalleri, A. Cavlin, V.K. Chadha, J.C. Chang, F.J. Charlson, H. Chen, W. Chen, Z. Chen, P.P. Chiang, O. Chimed-Ochir, R. Chowdhury, C.A. Christophi, T.W. Chuang, S.S. Chugh, M. Cirillo, T.K. Classen, V. Colistro, M. Colomar, S.M. Colquhoun, A.G. Contreras, C. Cooper, K. Cooperrider, L.T. Cooper, J. Coresh, K.J. Courville, M.H. Criqui, L. Cuevas-Nasu, J. Damsere-Derry, H. Danawi, L. Dandona, R. Dandona, P.I. Dargan, A. Davis, D.V. Davitoiu, A. Dayama, E.F. de Castro, V. De la Cruz-Gongora, D. De Leo, G. de Lima, L. Degenhardt, B. del Pozo-Cruz, R.P. Dellavalle, K. Deribe, S. Derrett, D.C. Des Jarlais, M. Dessalegn, G.A. deVeber, K.M. Devries, S.D. Dharmaratne, M.K. Dherani, D. Dicker, E.L. Ding, K. Dokova, E.R. Dorsey, T.R. Driscoll, L. Duan, A.M. Durrani, B.E. Ebel, R.G. Ellenbogen, Y.M. Elshrek, M. Endres, S.P. Ermakov, H.E. Erskine, B. Eshrati, A. Esteghamati, S. Fahimi, E.J. Faraon, F. Farzadfar, D.F. Fay, V.L. Feigin, A.B. Feigl, S.M. Fereshtehnejad, A.J. Ferrari, C.P. Ferri, A.D. Flaxman, T.D. Fleming, N. Foigt, K.J. Foreman, U.F. Paleo, R.C. Franklin, B. Gabbe, L. Gaffikin, E. Gakidou, A. Gamkrelidze, F.G. Gankpe, R.T. Gansevoort, F.A. Garcia-Guerra, E. Gasana, J.M. Geleijnse, B.D. Gessner, P. Gething, K.B. Gibney, R.F. Gillum, I.A. Ginawi, M. Giroud, G. Giussani, S. Goenka, K. Goginashvili, H. Gomez Dantes, P. Gona, T. Gonzalez de Cosio, D. Gonzalez-Castell, C.C. Gotay, A. Goto, H.N. Gouda, R.L. Guerrant, H.C. Gugnani, F. Guillemin, D. Gunnell, R. Gupta, R. Gupta, R.A. Gutierrez, N. Hafezi-Nejad, H. Hagan, M. Hagstromer, Y.A. Halasa, R.R. Hamadeh, M. Hammami, G.J. Hankey, Y. Hao, H.L. Harb, T.N. Haregu, J.M. Haro, R. Havmoeller, S.I. Hay, M.T. Hedayati, I.B. Heredia-Pi, L. Hernandez, K.R. Heuton, P. Heydarpour, M. Hijar, H.W. Hoek, H.J. Hoffman, J.C. Hornberger, H.D. Hosgood, D.G. Hoy, M. Hsairi, G. Hu, H. Hu, C. Huang, J.J. Huang, B.J. Hubbell, L. Huiart, A. Husseini, M.L. Iannarone, K.M. Iburg, B.T. Idrisov, N. Ikeda, K. Innos, M. Inoue, F. Islami, S. Ismayilova, K.H. Jacobsen, H.A. Jansen, D.L. Jarvis, S.K. Jassal, A. Jauregui, S. Jayaraman, P. Jeemon, P.N. Jensen, V. Jha, F. Jiang, G. Jiang, Y. Jiang, J.B. Jonas, K. Juel, H. Kan, S.S. Kany Roseline, N.E. Karam, A. Karch, C.K. Karema, G. Karthikeyan, A. Kaul, N. Kawakami, D.S. Kazi, A.H. Kemp, A.P. Kengne, A. Keren, Y.S. Khader, S.E. Khalifa, E.A. Khan, Y.H. Khang, S. Khatibzadeh, I. Khonelidze, C. Kieling, D. Kim, S. Kim, Y. Kim, R.W. Kimokoti, Y. Kinfu, J.M. Kinge, B.M. Kissela, M. Kivipelto, L.D. Knibbs, A.K. Knudsen, Y. Kokubo, M.R. Kose, S. Kosen, A. Kraemer, M. Kravchenko, S. Krishnaswami, H. Kromhout, T. Ku, B. Kuate Defo, B. Kucuk Bicer, E.J. Kuipers, C. Kulkarni, V.S. Kulkarni, G.A. Kumar, G.F. Kwan, T. Lai, A. Lakshmana Balaji, R. Lalloo, T. Lallukka, H. Lam, Q. Lan, V.C. Lansingh, H.J. Larson, A. Larsson, D.O. Laryea, P.M. Lavados, A.E. Lawrynowicz, J.L. Leasher, J.T. Lee, J. Leigh, R. Leung, M. Levi, Y. Li, Y. Li, J. Liang, X. Liang, S.S. Lim, M.P. Lindsay, S.E. Lipshultz, S. Liu, Y. Liu, B.K. Lloyd, G. Logroscino, S.J. London, N. Lopez, J. Lortet-Tieulent, P.A. Lotufo, R. Lozano, R. Lunevicius, J. Ma, S. Ma, V.M. Machado, M.F. MacIntyre, C. Magis-Rodriguez, A.A. Mahdi, M. Majdan, R. Malekzadeh, S. Mangalam, C.C. Mapoma, M. Marape, W. Marcenes, D.J. Margolis, C. Margono, G.B. Marks, R.V. Martin, M.B. Marzan, M.T. Mashal, F. Masiye, A.J. Mason-Jones, K. Matsushita, R. Matzopoulos, B.M. Mayosi, T.T. Mazorodze, A.C. McKay, M. McKee, A. McLain, P.A. Meaney, C. Medina, M.M. Mehndiratta, F. Mejia-Rodriguez, W. Mekonnen, Y.A. Melaku, M. Meltzer, Z.A. Memish, W. Mendoza, G.A. Mensah, A. Meretoja, F.A. Mhimbira, R. Micha, T.R. Miller, E.J. Mills, A. Misganaw, S. Mishra, N. Mohamed Ibrahim, K.A. Mohammad, A.H. Mokdad, G.L. Mola, L. Monasta, J.C. Montanez Hernandez, M. Montico, A.R. Moore, L. Morawska, R. Mori, J. Moschandreas, W.N. Moturi, D. Mozaffarian, U.O. Mueller, M. Mukaigawara, E.C. Mullany, K.S. Murthy, M. Naghavi, Z. Nahas, A. Naheed, K.S. Naidoo, L. Naldi, D. Nand, V. Nangia, K.M. Narayan, D. Nash, B. Neal, C. Nejjari, S.P. Neupane, C.R. Newton, F.N. Ngalesoni, D. Ngirabega Jde, G. Nguyen, N.T. Nguyen, M.J. Nieuwenhuijsen, M.I. Nisar, J.R. Nogueira, J.M. Nolla, S. Nolte, O.F. Norheim, R.E. Norman, B. Norrving, L. Nyakarahuka, I.H. Oh, T. Ohkubo, B.O. Olusanya, S.B. Omer, J.N. Opio, R. Orozco, R.S. Pagcatipunan Jr., A.W. Pain, J.D. Pandian, C.I. Panelo, C. Papachristou, E.K. Park, C.D. Parry, A.J. Paternina Caicedo, S.B. Patten, V.K. Paul, B.I. Pavlin, N. Pearce, L.S. Pedraza, A. Pedroza, L. Pejin Stokic, A. Pekericli, D.M. Pereira, R. Perez-Padilla, F. Perez-Ruiz, N. Perico, S.A. Perry, A. Pervaiz, K. Pesudovs, C.B. Peterson, M. Petzold, M.R. Phillips, H.P. Phua, D. Plass, D. Poenaru, G.V. Polanczyk, S. Polinder, C.D. Pond, C.A. Pope, D. Pope, S. Popova, F. Pourmalek, J. Powles, D. Prabhakaran, N.M. Prasad, D.M. Qato, A.D. Quezada, D.A. Quistberg, L. Racape, A. Rafay, K. Rahimi, V. Rahimi-Movaghar, S.U. Rahman, M. Raju, I. Rakovac, S.M. Rana, M. Rao, H. Razavi, K.S. Reddy, A.H. Refaat, J. Rehm, G. Remuzzi, A.L. Ribeiro, P.M. Riccio, L. Richardson, A. Riederer, M. Robinson, A. Roca, A. Rodriguez, D. Rojas-Rueda, I. Romieu, L. Ronfani, R. Room, N. Roy, G.M. Ruhago, L. Rushton, N. Sabin, R.L. Sacco, S. Saha, R. Sahathevan, M.A. Sahraian, J.A. Salomon, D. Salvo, U.K. Sampson, J.R. Sanabria, L.M. Sanchez, T.G. Sanchez-Pimienta, L. Sanchez-Riera, L. Sandar, I.S. Santos, A. Sapkota, M. Satpathy, J.E. Saunders, M. Sawhney, M.I. Saylan, P. Scarborough, J.C. Schmidt, I.J. Schneider, B. Schottker, D.C. Schwebel, J.G. Scott, S. Seedat, S.G. Sepanlou, B. Serdar, E.E. Servan-Mori, G. Shaddick, S. Shahraz, T.S. Levy, S. Shangguan, J. She, S. Sheikhbahaei, K. Shibuya, H.H. Shin, Y. Shinohara, R. Shiri, K. Shishani, I. Shiue, I.D. Sigfusdottir, D.H. Silberberg, E.P. Simard, S. Sindi, A. Singh, G.M. Singh, J.A. Singh, V. Skirbekk, K. Sliwa, M. Soljak, S. Soneji, K. Soreide, S. Soshnikov, L.A. Sposato, C.T. Sreeramareddy, N.J. Stapelberg, V. Stathopoulou, N. Steckling, D.J. Stein, M.B. Stein, N. Stephens, H. Stockl, K. Straif, K. Stroumpoulis, L. Sturua, B.F. Sunguya, S. Swaminathan, M. Swaroop, B.L. Sykes, K.M. Tabb, K. Takahashi, R.T. Talongwa, N. Tandon, D. Tanne, M. Tanner, M. Tavakkoli, B.J. Te Ao, C.M. Teixeira, M.M. Tellez Rojo, A.S. Terkawi, J.L. Texcalac-Sangrador, S.V. Thackway, B. Thomson, A.L. Thorne-Lyman, A.G. Thrift, G.D. Thurston, T. Tillmann, M. Tobollik, M. Tonelli, F. Topouzis, J.A. Towbin, H. Toyoshima, J. Traebert, B.X. Tran, L. Trasande, M. Trillini, U. Trujillo, Z.T. Dimbuene, M. Tsilimbaris, E.M. Tuzcu, U.S. Uchendu, K.N. Ukwaja, S.B. Uzun, S. van de Vijver, R. Van Dingenen, C.H. van Gool, J. van Os, Y.Y. Varakin, T.J. Vasankari, A.M. Vasconcelos, M.S. Vavilala, L.J. Veerman, G. Velasquez-Melendez, N. Venketasubramanian, L. Vijayakumar, S. Villalpando, F.S. Violante, V.V. Vlassov, S.E. Vollset, G.R. Wagner, S.G. Waller, M.T. Wallin, X. Wan, H. Wang, J. Wang, L. Wang, W. Wang, Y. Wang, T.S. Warouw, C.H. Watts, S. Weichenthal, E. Weiderpass, R.G. Weintraub, A. Werdecker, K.R. Wessells, R. Westerman, H.A. Whiteford, J.D. Wilkinson, H.C. Williams, T.N. Williams, S.M. Woldeyohannes, C.D. Wolfe, J.Q. Wong, A.D. Woolf, J.L. Wright, B. Wurtz, G. Xu, L.L. Yan, G. Yang, Y. Yano, P. Ye, M. Yenesew, G.K. Yentur, P. Yip, N. Yonemoto, S.J. Yoon, M.Z. Younis, Z. Younoussi, C. Yu, M.E. Zaki, Y. Zhao, Y. Zheng, M. Zhou, J. Zhu, S. Zhu, X. Zou, J.R. Zunt, A.D. Lopez, T. Vos, C.J. Murray, Global, regional, and national comparative risk assessment of 79 behavioural, environmental and occupational, and metabolic risks or clusters of risks in 188 countries, 1990–2013: a systematic analysis for the Global Burden of Disease Study 2013, Lancet 386 (2015) 2287–2323.

[7] A. American Diabetes, Economic costs of diabetes in the U.S. in 2012, Diabetes Care 36 (2013) 1033–1046.

[8] A. Ott, R.P. Stolk, F. van Harskamp, H.A. Pols, A. Hofman, M.M. Breteler, Diabetes mellitus and the risk of dementia: the Rotterdam Study, Neurology 53 (1999) 1937–1942.

[9] R. Peila, B.L. Rodriguez, L.J. Launer, S. Honolulu-Asia Aging, Type 2 diabetes, APOE gene, and the risk for dementia and related pathologies: the Honolulu-Asia Aging Study, Diabetes 51 (2002) 1256–1262.

[10] Z. Arvanitakis, R.S. Wilson, J.L. Bienias, D.A. Evans, D.A. Bennett, Diabetes mellitus and risk of Alzheimer disease and decline in cognitive function, Arch. Neurol. 61 (2004) 661–666.

[11] J.A. Luchsinger, C. Reitz, L.S. Honig, M.X. Tang, S. Shea, R. Mayeux, Aggregation of vascular risk factors and risk of incident Alzheimer disease, Neurology 65 (2005) 545–551.

[12] G.J. Biessels, S. Staekenborg, E. Brunner, C. Brayne, P. Scheltens, Risk of dementia in diabetes mellitus: a systematic review, Lancet Neurol. 5 (2006) 64–74.

[13] F. Irie, A.L. Fitzpatrick, O.L. Lopez, L.H. Kuller, R. Peila, A.B. Newman, L.J. Launer, Enhanced risk for Alzheimer disease in persons with type 2 diabetes and APOE epsilon4: the Cardiovascular Health Study Cognition Study, Arch. Neurol. 65 (2008) 89–93.

[14] S. Ahtiluoto, T. Polvikoski, M. Peltonen, A. Solomon, J. Tuomilehto, B. Winblad, R. Sulkava, M. Kivipelto, Diabetes, Alzheimer disease, and vascular dementia: a population-based neuropathologic study, Neurology 75 (2010) 1195–1202.

[15] N.T. Vagelatos, G.D. Eslick, Type 2 diabetes as a risk factor for Alzheimer's disease: the confounders, interactions, and neuropathology associated with this relationship, Epidemiol. Rev. 35 (2013) 152–160.

[16] J.D. Voss, R.L. Atkinson, N.V. Dhurandhar, Role of adenoviruses in obesity, Rev. Med. Virol. 25 (2015) 379–387.

[17] N.V. Dhurandhar, A framework for identification of infections that contribute to human obesity, Lancet Infect. Dis. 11 (2011) 963–969.

[18] M. Akheruzzaman, V. Hegde, N.V. Dhurandhar, Twenty-five years of research about adipogenic adenoviruses: a systematic review, Obes. Rev. 20 (2019) 499–509.

[19] M. Pasarica, A.C. Shin, M. Yu, H.M. Ou Yang, M. Rathod, K.L. Jen, S. MohanKumar, P.S. MohanKumar, N. Markward, N.V. Dhurandhar, Human adenovirus 36 induces adiposity, increases insulin sensitivity, and alters hypothalamic monoamines in rats, Obesity (Silver Spring) 14 (2006) 1905–1913.

[20] R. Krishnapuram, E.J. Dhurandhar, O. Dubuisson, H. Kirk-Ballard, S. Bajpeyi, N. Butte, M.S. Sothern, E. Larsen-Meyer, S. Chalew, B. Bennett, A.K. Gupta, F.L. Greenway, W. Johnson, M. Brashear, G. Reinhart, T. Rankinen, C. Bouchard, W.T. Cefalu, J. Ye, R. Javier, A. Zuberi, N.V. Dhurandhar, Template to improve glycemic control without reducing adiposity or dietary fat, Am. J. Physiol. Endocrinol. Metab. 300 (2011) E779–E789.

[21] M. Manczak, R. Kandimalla, D. Fry, H. Sesaki, P.H. Reddy, Protective effects of reduced dynamin-related protein 1 against amyloid beta-induced mitochondrial dysfunction and synaptic damage in Alzheimer's disease, Hum. Mol. Genet. 25 (2016) 5148–5166.

[22] N.V. Dhurandhar, B.A. Israel, J.M. Kolesar, G. Mayhew, M.E. Cook, R.L. Atkinson, Transmissibility of adenovirus-induced adiposity in a chicken model, Int. J. Obes. Relat. Metab. Disord. 25 (2001) 990–996.

[23] N.V. Dhurandhar, B.A. Israel, J.M. Kolesar, G.F. Mayhew, M.E. Cook, R.L. Atkinson, Increased adiposity in animals due to a human virus, Int. J. Obes. Relat. Metab. Disord. 24 (2000) 989–996.

[24] R. Gibb, B. Kolb, A method for vibratome sectioning of Golgi-Cox stained whole rat brain, J. Neurosci. Methods 79 (1998) 1–4.

[25] A. Ott, R.P. Stolk, A. Hofman, F. van Harskamp, D.E. Grobbee, M.M. Breteler, Association of diabetes mellitus and dementia: the Rotterdam Study, Diabetologia 39 (1996) 1392–1397.

[26] C.L. Leibson, W.A. Rocca, V.A. Hanson, R. Cha, E. Kokmen, P.C. O'Brien, P.J. Palumbo, Risk of dementia among persons with diabetes mellitus: a population-based cohort study, Am. J. Epidemiol. 145 (1997) 301–308.

[27] E. Ronnemaa, B. Zethelius, J. Sundelof, J. Sundstrom, M. Degerman-Gunnarsson, C. Berne, L. Lannfelt, L. Kilander, Impaired insulin secretion increases the risk of Alzheimer disease, Neurology 71 (2008) 1065–1071.

[28] A.A. Willette, S.C. Johnson, A.C. Birdsill, M.A. Sager, B. Christian, L.D. Baker, S. Craft, J. Oh, E. Statz, B.P. Hermann, E.M. Jonaitis, R.L. Koscik, A. La Rue,

S. Asthana, B.B. Bendlin, Insulin resistance predicts brain amyloid deposition in late middle-aged adults, Alzheimers Dement. 11 (2015) 504–510 (e501).
[29] G. Bedse, F. Di Domenico, G. Serviddio, T. Cassano, Aberrant insulin signaling in Alzheimer's disease: current knowledge, Front. Neurosci. 9 (2015) 204.
[30] K. Morgen, L. Frolich, The metabolism hypothesis of Alzheimer's disease: from the concept of central insulin resistance and associated consequences to insulin therapy, J. Neural Transm. (Vienna) 122 (2015) 499–504.
[31] E. Steen, B.M. Terry, E.J. Rivera, J.L. Cannon, T.R. Neely, R. Tavares, X.J. Xu, J.R. Wands, S.M. de la Monte, Impaired insulin and insulin-like growth factor expression and signaling mechanisms in Alzheimer's disease—is this type 3 diabetes? J. Alzheimers Dis. 7 (2005) 63–80.
[32] J.A. Sonnen, E.B. Larson, K. Brickell, P.K. Crane, R. Woltjer, T.J. Montine, S. Craft, Different patterns of cerebral injury in dementia with or without diabetes, Arch. Neurol. 66 (2009) 315–322.
[33] T. Valente, A. Gella, X. Fernandez-Busquets, M. Unzeta, N. Durany, Immunohistochemical analysis of human brain suggests pathological synergism of Alzheimer's disease and diabetes mellitus, Neurobiol. Dis. 37 (2010) 67–76.
[34] G.J. Biessels, I.J. Deary, C.M. Ryan, Cognition and diabetes: a lifespan perspective, Lancet Neurol. 7 (2008) 184–190.
[35] R. Krishnapuram, H. Kirk-Ballard, E.J. Dhurandhar, O. Dubuisson, V. Messier, R. Rabasa-Lhoret, V. Hegde, S. Aggarwal, N.V. Dhurandhar, Insulin receptor-independent upregulation of cellular glucose uptake, Int. J. Obes. 37 (2013) 146–153.
[36] S.M. Clee, A.D. Attie, The genetic landscape of type 2 diabetes in mice, Endocr. Rev. 28 (2007) 48–83.
[37] D.A. Fontaine, D.B. Davis, Attention to background strain is essential for metabolic research: C57BL/6 and the International Knockout Mouse Consortium, Diabetes 65 (2016) 25–33.
[38] L. Gimenez-Llort, Y. Garcia, K. Buccieri, S. Revilla, C. Sunol, R. Cristofol, C. Sanfeliu, Gender-specific neuroimmunoendocrine response to treadmill exercise in 3xTg-AD mice, Int. J. Alzheimers Dis. 2010 (2010) 128354.
[39] H.G. Joost, A. Schurmann, The genetic basis of obesity-associated type 2 diabetes (diabesity) in polygenic mouse models, Mamm. Genome 25 (2014) 401–412.
[40] I. Pedros, D. Petrov, M. Allgaier, F. Sureda, E. Barroso, C. Beas-Zarate, C. Auladell, M. Pallas, M. Vazquez-Carrera, G. Casadesus, J. Folch, A. Camins, Early alterations in energy metabolism in the hippocampus of APPswe/PS1dE9 mouse model of Alzheimer's disease, Biochim. Biophys. Acta 1842 (2014) 1556–1566.
[41] S. Takeda, N. Sato, K. Uchio-Yamada, K. Sawada, T. Kunieda, D. Takeuchi, H. Kurinami, M. Shinohara, H. Rakugi, R. Morishita, Elevation of plasma beta-amyloid level by glucose loading in Alzheimer mouse models, Biochem. Biophys. Res. Commun. 385 (2009) 193–197.
[42] M. Vandal, P.J. White, G. Chevrier, C. Tremblay, I. St-Amour, E. Planel, A. Marette, F. Calon, Age-dependent impairment of glucose tolerance in the 3xTg-AD mouse model of Alzheimer's disease, FASEB J. 29 (2015) 4273–4284.
[43] Y. Zhang, B. Zhou, F. Zhang, J. Wu, Y. Hu, Y. Liu, Q. Zhai, Amyloid-beta induces hepatic insulin resistance by activating JAK2/STAT3/SOCS-1 signaling pathway, Diabetes 61 (2012) 1434–1443.
[44] L. Macklin, C.M. Griffith, Y. Cai, G.M. Rose, X.X. Yan, P.R. Patrylo, Glucose tolerance and insulin sensitivity are impaired in APP/PS1 transgenic mice prior to amyloid plaque pathogenesis and cognitive decline, Exp. Gerontol. 88 (2017) 9–18.
[45] N. Wijesekara, R. Ahrens, M. Sabale, L. Wu, K. Ha, G. Verdile, P.E. Fraser, Amyloid-beta and islet amyloid pathologies link Alzheimer's disease and type 2 diabetes in a transgenic model, FASEB J. 31 (2017) 5409–5418.
[46] J.C. Bruning, D. Gautam, D.J. Burks, J. Gillette, M. Schubert, P.C. Orban, R. Klein, W. Krone, D. Muller-Wieland, C.R. Kahn, Role of brain insulin receptor in control of body weight and reproduction, Science 289 (2000) 2122–2125.
[47] L. Schmitz, R. Kuglin, I. Bae-Gartz, R. Janoschek, S. Appel, A. Mesaros, I. Jakovcevski, C. Vohlen, M. Handwerk, R. Ensenauer, J. Dotsch, E. Hucklenbruch-Rother, Hippocampal insulin resistance links maternal obesity with impaired neuronal plasticity in adult offspring, Psychoneuroendocrinology 89 (2018) 46–52.
[48] Q. Wan, Z.G. Xiong, H.Y. Man, C.A. Ackerley, J. Braunton, W.Y. Lu, L.E. Becker, J.F. MacDonald, Y.T. Wang, Recruitment of functional GABA(A) receptors to postsynaptic domains by insulin, Nature 388 (1997) 686–690.
[49] C.R. Park, R.J. Seeley, S. Craft, S.C. Woods, Intracerebroventricular insulin enhances memory in a passive-avoidance task, Physiol. Behav. 68 (2000) 509–514.
[50] C. Benedict, W. Kern, B. Schultes, J. Born, M. Hallschmid, Differential sensitivity of men and women to anorexigenic and memory-improving effects of intranasal insulin, J. Clin. Endocrinol. Metab. 93 (2008) 1339–1344.
[51] S.M. de la Monte, Contributions of brain insulin resistance and deficiency in amyloid-related neurodegeneration in Alzheimer's disease, Drugs 72 (2012) 49–66.
[52] K. Talbot, H.Y. Wang, H. Kazi, L.Y. Han, K.P. Bakshi, A. Stucky, R.L. Fuino, K.R. Kawaguchi, A.J. Samoyedny, R.S. Wilson, Z. Arvanitakis, J.A. Schneider, B.A. Wolf, D.A. Bennett, J.Q. Trojanowski, S.E. Arnold, Demonstrated brain insulin resistance in Alzheimer's disease patients is associated with IGF-1 resistance, IRS-1 dysregulation, and cognitive decline, J. Clin. Invest. 122 (2012) 1316–1338.
[53] H. Umegaki, Insulin resistance in the brain: a new therapeutic target for Alzheimer's disease, J. Diabetes Investig. 4 (2013) 150–151.
[54] J. Hardy, D.J. Selkoe, The amyloid hypothesis of Alzheimer's disease: progress and problems on the road to therapeutics, Science 297 (2002) 353–356.
[55] H.A. Pearson, C. Peers, Physiological roles for amyloid beta peptides, J. Physiol. 575 (2006) 5–10.
[56] J. Greenwald, R. Riek, Biology of amyloid: structure, function, and regulation, Structure 18 (2010) 1244–1260.
[57] K. Blennow, Cerebrospinal fluid protein biomarkers for Alzheimer's disease, NeuroRx 1 (2004) 213–225.
[58] F. Du, Q. Yu, S. Yan, G. Hu, L.F. Lue, D.G. Walker, L. Wu, S.F. Yan, K. Tieu, S.S. Yan, PINK1 signalling rescues amyloid pathology and mitochondrial dysfunction in Alzheimer's disease, Brain 140 (2017) 3233–3251.
[59] T. Rush, J. Martinez-Hernandez, M. Dollmeyer, M.L. Frandemiche, E. Borel, S. Boisseau, M. Jacquier-Sarlin, A. Buisson, Synaptotoxicity in Alzheimer's disease involved a dysregulation of actin cytoskeleton dynamics through cofilin 1 phosphorylation, J. Neurosci. 38 (2018) 10349–10361.
[60] B.D. Boros, K.M. Greathouse, E.G. Gentry, K.A. Curtis, E.L. Birchall, M. Gearing, J.H. Herskowitz, Dendritic spines provide cognitive resilience against Alzheimer's disease, Ann. Neurol. 82 (2017) 602–614.
[61] T. Spires-Jones, S. Knafo, Spines, plasticity, and cognition in Alzheimer's model mice, Neural. Plast. 2012 (2012) 319836.
[62] W. Zhao, H. Chen, H. Xu, E. Moore, N. Meiri, M.J. Quon, D.L. Alkon, Brain insulin receptors and spatial memory. Correlated changes in gene expression, tyrosine phosphorylation, and signaling molecules in the hippocampus of water maze trained rats, J. Biol. Chem. 274 (1999) 34893–34902.
[63] R.S. Zimmerman, T.M. Hobbs, B.J. Wells, S.X. Kong, M.W. Kattan, J. Bouchard, K.M. Chagin, C. Yu, B. Sakurada, A. Milinovich, W. Weng, J.M. Bauman, K.M. Pantalone, Association of glucagon-like peptide-1 receptor agonist use and rates of acute myocardial infarction, stroke and overall mortality in patients with type 2 diabetes mellitus in a large integrated health system, Diabetes Obes. Metab. 19 (2017) 1555–1561.
[64] S. Craft, A. Claxton, L.D. Baker, A.J. Hanson, B. Cholerton, E.H. Trittschuh, D. Dahl, E. Caulder, B. Neth, T.J. Montine, Y. Jung, J. Maldjian, C. Whitlow, S. Friedman, Effects of regular and long-acting insulin on cognition and Alzheimer's disease biomarkers: a pilot clinical trial, J. Alzheimers Dis. 57 (2017) 1325–1334.
[65] J. Sanahuja, N. Alonso, J. Diez, E. Ortega, E. Rubinat, A. Traveset, N. Alcubierre, A. Betriu, E. Castelblanco, M. Hernandez, F. Purroy, M.V. Arcidiacono, C. Jurjo, E. Fernandez, M. Puig-Domingo, P.H. Groop, D. Mauricio, Increased burden of cerebral small vessel disease in patients with type 2 diabetes and retinopathy, Diabetes Care 39 (2016) 1614–1620.
[66] S. Craft, S. Asthana, D.G. Cook, L.D. Baker, M. Cherrier, K. Purganan, C. Wait, A. Petrova, S. Latendresse, G.S. Watson, J.W. Newcomer, G.D. Schellenberg, A.J. Krohn, Insulin dose-response effects on memory and plasma amyloid precursor protein in Alzheimer's disease: interactions with apolipoprotein E genotype, Psychoneuroendocrinology 28 (2003) 809–822.
[67] S. Craft, G.S. Watson, Insulin and neurodegenerative disease: shared and specific mechanisms, Lancet Neurol. 3 (2004) 169–178.
[68] R. Ravona-Springer, X. Luo, J. Schmeidler, M. Wysocki, G. Lesser, M. Rapp, K. Dahlman, H. Grossman, V. Haroutunian, M. Schnaider Beeri, Diabetes is associated with increased rate of cognitive decline in questionably demented elderly, Dement. Geriatr. Cogn. Disord. 29 (2010) 68–74.
[69] Z.Q. Wang, W.T. Cefalu, X.H. Zhang, Y. Yu, J. Qin, L. Son, P.M. Rogers, N. Mashtalir, J.R. Bordelon, J. Ye, N.V. Dhurandhar, Human adenovirus type 36 enhances glucose uptake in diabetic and nondiabetic human skeletal muscle cells independent of insulin signaling, Diabetes 57 (2008) 1805–1813.
[76] W.Y. Lin, O. Dubuisson, R. Rubicz, N. Liu, D.B. Allison, J.E. Curran, A.G. Comuzzie, J. Blangero, C.T. Leach, H. Goring, N.V. Dhurandhar, Long-term changes in adiposity and glycemic control are associated with past adenovirus infection, Diabetes Care 36 (2013) 701–707.
[77] M. Pasarica, N. Mashtalir, E.J. McAllister, G.E. Kilroy, J. Koska, P. Permana, B. de Courten, M. Yu, E. Ravussin, J.M. Gimble, N.V. Dhurandhar, Adipogenic human adenovirus Ad-36 induces commitment, differentiation, and lipid accumulation in human adipose-derived stem cells, Stem Cells. 26 (4) (2008) 969–978, https://doi.org/10.1634/stemcells.2007-0868.